

Natural Variation in Small Molecule–Induced TIR-NB-LRR Signaling Induces Root Growth Arrest via EDS1- and PAD4-Complexed R Protein VICTR in *Arabidopsis*

Tae-Houn Kim,^{a,1} Hans-Henning Kunz,^a Saikat Bhattacharjee,^b Felix Hauser,^a Jiyoun Park,^a Cawas Engineer,^a Amy Liu,^a Tracy Ha,^a Jane E. Parker,^c Walter Gassmann,^b and Julian I. Schroeder^{a,2}

^a Division of Biological Sciences, Section of Cell and Developmental Biology, University of California at San Diego, La Jolla, California 92093-0116

^b Division of Plant Sciences, Christopher S. Bond Life Sciences Center and Interdisciplinary Plant Group, University of Missouri, Columbia, Missouri 65211-7310

^c Max-Planck Institute for Plant Breeding Research, Department of Plant-Microbe Interactions, D-50829 Cologne, Germany

In a chemical genetics screen we identified the small-molecule [5-(3,4-dichlorophenyl)furan-2-yl]-piperidine-1-ylmethanethione (DFPM) that triggers rapid inhibition of early abscisic acid signal transduction via PHYTOALEXIN DEFICIENT4 (PAD4)- and ENHANCED DISEASE SUSCEPTIBILITY1 (EDS1)-dependent immune signaling mechanisms. However, mechanisms upstream of EDS1 and PAD4 in DFPM-mediated signaling remain unknown. Here, we report that DFPM generates an *Arabidopsis thaliana* accession-specific root growth arrest in Columbia-0 (Col-0) plants. The genetic locus responsible for this natural variant, *VICTR* (VARIATION IN COMPOUND TRIGGERED ROOT growth response), encodes a TIR-NB-LRR (for Toll-Interleukin1 Receptor–nucleotide binding–Leucine-rich repeat) protein. Analyses of T-DNA insertion *vict*r alleles showed that *VICTR* is necessary for DFPM-induced root growth arrest and inhibition of abscisic acid–induced stomatal closing. Transgenic expression of the Col-0 *VICTR* allele in DFPM-insensitive *Arabidopsis* accessions recapitulated the DFPM-induced root growth arrest. *EDS1* and *PAD4*, both central regulators of basal resistance and effector-triggered immunity, as well as *HSP90* chaperones and their cochaperones *RAR1* and *SGT1B*, are required for the DFPM-induced root growth arrest. Salicylic acid and jasmonic acid signaling pathway components are dispensable. We further demonstrate that *VICTR* associates with *EDS1* and *PAD4* in a nuclear protein complex. These findings show a previously unexplored association between a TIR-NB-LRR protein and *PAD4* and identify functions of plant immune signaling components in the regulation of root meristematic zone-targeted growth arrest.

INTRODUCTION

Chemical genetics provides a powerful tool to address redundancy and network robustness in signal transduction (Schreiber, 2000; Armstrong et al., 2004; Zouhar et al., 2004; Park et al., 2009). In a recent screen of a 9600-compound chemical library for inhibition of abscisic acid (ABA) signaling, a small molecule named [5-(3,4-dichlorophenyl)furan-2-yl]-piperidine-1-ylmethanethione (DFPM) was isolated that showed the capacity to inhibit several ABA responses, including rapid disruption of ABA-induced stomatal closing and ABA activation of guard cell anion channels (Kim et al., 2011). Detailed analyses revealed that DFPM stimulates an effector-triggered immune

signaling pathway and thereby rapidly disrupts ABA signal transduction (Kim et al., 2011).

The central regulators of basal resistance and effector-triggered immunity, *EDS1* and *PAD4*, as well as the cochaperones *RAR1* (REQUIRED FOR Mla12 RESISTANCE) and *SGT1b* (SUPPRESSOR OF G-TWO ALLELE OF SKP1b) are required for DFPM-induced disruption of ABA signaling (Kim et al., 2011). Effector-triggered immunity relies on resistance (R) proteins as sensors that indirectly or directly recognize specific pathogen-derived effector molecules and trigger downstream disease resistance responses (Glazebrook, 2005; Jones and Dangl, 2006). Whether specific R proteins are required for the small-molecule DFPM-induced response remains unknown. Depending on their N-terminal domain, R proteins are generally divided into two groups, coiled-coil (CC)-nucleotide binding (NB)-leucine-rich repeat (LRR) and Toll-Interleukin1 Receptor (TIR)-NB-LRR (Meyers et al., 2003; Belkadir et al., 2004; Chisholm et al., 2006; DeYoung and Innes, 2006; Shen and Schulze-Lefert, 2007; Caplan et al., 2008). The genome of *Arabidopsis thaliana* contains ~150 *NB-LRR* genes, and up to 600 genes are found in rice (*Oryza sativa*; Kadota et al., 2010). The presence of many polymorphisms in *NB-LRR* genes has been proposed as a diversification process against rapidly evolving pathogens (Tian et al., 2003; Guo et al., 2011). In fact, *NB-LRR* genes represent the most variable plant gene family (Weigel, 2012).

¹ Current address: College of Natural Sciences, Duksung Women's University, 132-714 Seoul, Korea.

² Address correspondence to jischroeder@ucsd.edu.

The author responsible for distribution of materials integral to the findings presented in this article in accordance with the policy described in the Instructions for Authors (www.plantcell.org) is: Julian I. Schroeder (jischroeder@ucsd.edu).

 Some figures in this article are displayed in color online but in black and white in the print edition.

 Online version contains Web-only data.

www.plantcell.org/cgi/doi/10.1105/tpc.112.107235

Upon pathogen recognition, intramolecular structural changes of NB-LRR proteins induce ADP-ATP exchange in the NB domain and activate downstream responses. Effector-triggered activation of TIR-NB-LRR proteins requires the function of EDS1 and PAD4 to generate downstream disease resistance responses, including salicylic acid-mediated signal transduction (Wiermer et al., 2005). Recently, it was found that EDS1 resides in some complexes with TIR-NB-LRR proteins (Bhattacharjee et al., 2011; Heidrich et al., 2011).

Here, using a chemical genetics approach, we identified natural genetic variation in a primary root growth response induced by the small molecule DFPM. The *Arabidopsis* Columbia-0 (Col-0) accession responds specifically to DFPM by generating a primary root meristem arrest. Molecular identification of the responsible genetic locus and its functional characterization demonstrate that a natural genetic variant in the *TIR-NB-LRR* gene *VICTR* (for *VARIATION IN COMPOUND TRIGGERED ROOT growth response*) determines DFPM-induced root growth arrest. Involvement of additional components of effector-triggered immune signaling in this phenotype implicates pathogen-induced primary root growth arrest as a possible resistance response to soil-borne plant pathogens. Furthermore, we show an association of *VICTR* protein with EDS1 and with PAD4 within a nuclear complex. The finding of PAD4 within a TIR-NB-LRR-containing protein complex expands recent findings that TIR-

NB-LRR R proteins can associate within complexes with the EDS1 protein (Bhattacharjee et al., 2011; Heidrich et al., 2011). The DFPM-induced PAD4- and EDS1-dependent root growth arrest is caused by inhibition of primary root meristem activity. The DFPM-induced and easily scored root growth arrest provides a powerful tool for further dissection of R protein/EDS1/PAD4-dependent signaling mechanisms, as genetic and cell biological components of immunity-induced cell death pathways can be identified, as shown here for *VICTR*.

RESULTS

Accession-Specific Primary Root Growth Response to the Small Compound DFPM

The chemical compound DFPM (Figure 1A) was isolated from a chemical library of 9600 compounds by screening for physiologically active small molecules that inhibit ABA-induced gene expression and signal transduction (Kim et al., 2011). An in-depth screen for additional visible phenotypic responses caused by DFPM application identified a rapid root growth inhibition after DFPM treatment. Intriguingly, this arrest was found to be specific for the Col-0 accession. DFPM did not affect root growth of the *Arabidopsis* Landsberg *erecta* (*Ler*) accession (Figure 1B). At a concentration of 5 μ M DFPM, root growth of

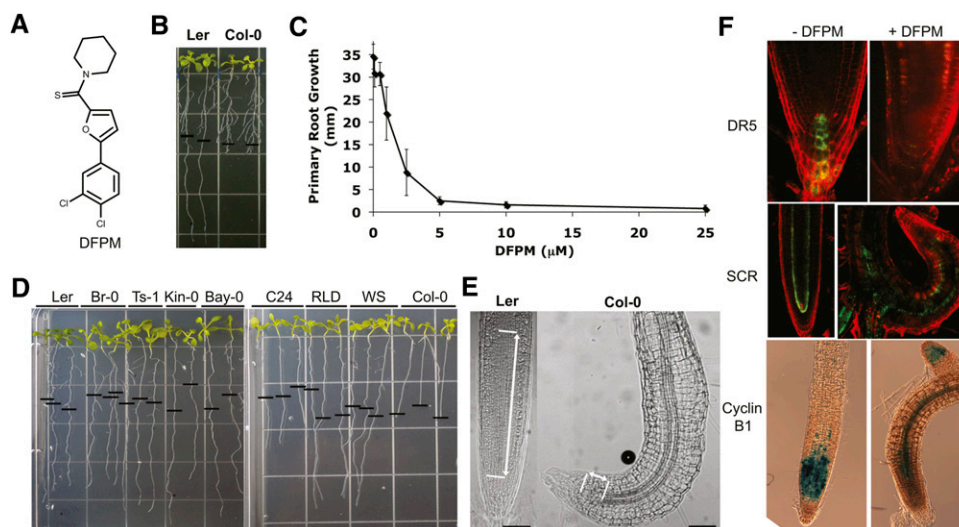


Figure 1. Natural Genetic Variation in Compound-Specific Root Growth Arrest Specifically Targets the Primary Root Meristem in Col-0.

(A) Chemical structure of root growth arrest-causing DFPM.

(B) DFPM causes a primary root growth arrest phenotype in Col-0.

(C) DFPM-induced root growth inhibition of Col-0 ($EC_{50} \sim 1.5 \mu$ M). Error bars mean \pm SD.

(D) While Col-0 roots are sensitive to DFPM, roots of *Ler*, Br-0 (Brunn-0), Ts-1 (Tossa de Mar-1), Kin-0 (Kindalville-0), Bay-0 (Bayreuth-0), C24, RLD (Rschew), WS (Wassilewskija), and 42 other *Arabidopsis* accessions (see Supplemental Table 1 online) produced no significant growth arrest response to DFPM. The black horizontal bars mark the starting position of roots when DFPM was applied.

(E) Microscopy examination of DFPM-treated roots reveals that while root differentiation is normal, meristematic and elongation zones of the primary root are reduced in size in response to DFPM in Col-0. Note that *Ler* produced normal root morphology in response to DFPM exposure (left). Meristematic and elongation zones are indicated by lines and arrows. Bars = 50 μ m.

(F) Deregulated *DR5* promoter expression by DFPM indicates that auxin accumulation is abrogated in the root meristem after 4 d of DFPM treatment. Expression of the endodermal marker gene *SCR* is also altered by DFPM. Expression of the *CyclinB1* promoter suggests that cell cycle activity in the DFPM-treated primary root tip is reduced. All marker lines tested here are in the Col-0 background.

Col-0 was blocked ($EC_{50} = 1.5 \mu\text{M}$; Figure 1C). The seedling root growth of 50 other *Arabidopsis* accessions, including *Ler*, Kindalville-0 (Kin-0), Bayreuth-0 (Bay-0), and C24, were not affected by DFPM treatment (Figure 1D; see Supplemental Table 1 online). We concluded that the Col-0 accession contains unusual natural genetic variation that causes DFPM-induced root growth arrest. Based on the phenotype, we refer to this class of genes as *VICTR*. In response to DFPM, primary root growth of Col-0 was abrogated, but secondary lateral root growth was not (Figure 1B).

Chemical compounds structurally similar to DFPM (see Supplemental Figure 1A online) were analyzed to define critical structural motifs required for the triggering of the *VICTR* phenotype. These analyses showed that modifications in the structure of several DFPM-related compounds can reduce the potency of the DFPM response. Although the slightly modified molecules DFPM-1 and DFPM-2 exhibited biological activity similar to the original DFPM, a chlorine in the four position seemed to be critical for eliciting the *VICTR* phenotype (see Supplemental Figure 1 online). Loss of activity was also caused by modifications of side groups as shown in DFPM-3. Whether DFPM or a breakdown product thereof is the active compound remains to be determined. The root growth response caused by DFPM was found to be time dependent. Only 8 h of DFPM treatment was sufficient to initiate the *VICTR* phenotype in an irreversible manner (see Supplemental Figure 2C online). Primary root growth did not recover even 6 d after seedlings were retransferred to standard growth media.

DFPM Targets the Primary Root Meristematic Zone in Col-0

Microscopy examination of the morphological changes of Col-0 roots treated with DFPM revealed a large reduction of the meristematic and elongation zones, whereas root differentiation, such as vascular and lateral root formation, did not show any observable differences, indicating that DFPM may target the primary root meristematic zone (Figure 1E). To investigate molecular changes in DFPM-treated primary root tips, the pattern of local auxin accumulation was examined using *DR5* promoter-driven green fluorescent protein (GFP) lines (Friml et al., 2003) in the Col-0 background (Figure 1F). DFPM treatment for 1 d did not change the *pDR5:GFP* activity at the columella at the root tip (see Supplemental Figure 2A online). After 4 d of DFPM treatment, no *pDR5:GFP* activity was visible at the columella of Col-0 (Figure 1F), consistent with the model that DFPM targets the primary root meristem. However, the *pDR5:GFP* construct has been reported to have certain limitations as an auxin reporter and to not necessarily correlate with other auxin-sensitive genes (Moreno-Risueno et al., 2010). Therefore, to measure the effect of DFPM on auxin transporters in the primary root, *pPIN1:PIN1-GFP* and *pPIN2:PIN2-GFP* Col-0 lines were monitored as a function of time after DFPM exposure (see Supplemental Figure 2B online). After 18 h of DFPM treatment, both PIN1:GFP and PIN2:GFP signals became weaker. At 24 h, when DFPM-mediated root growth arrest becomes visible, both PIN1:GFP and PIN2:GFP levels decreased substantially. These results indicate that altered PIN1 or PIN2 activities and resulting changes in the auxin gradient, which is important to maintain meristematic cell divisions (Bliou et al., 2005; Dello Iorio et al., 2007; Fernández-

Marcos et al., 2011), might contribute to DFPM-mediated root growth inhibition.

SCARECROW (SCR) expression was analyzed as an endodermal and quiescent center marker gene (Di Lorenzo et al., 1996). *SCR* expression was disrupted after 4 d of DFPM treatment when DFPM had already produced obvious morphological differences (Figure 1F). However, *SCR* expression exhibited a normal pattern of expression after 1 d of DFPM treatment (see Supplemental Figure 2A online). Therefore, the disrupted *SCR* expression in Col-0 might be a secondary effect of the altered root morphology after DFPM treatment.

Consistent with the deregulated *DR5* and *SCR* expression patterns induced after 4 d by DFPM, cell cycle activity monitored by the *Cyclin B1* promoter (Colón-Carmona et al., 1999) was disrupted by DFPM treatment (Figure 1F). Retention of the normal expression pattern of *Cyclin B1* in secondary root meristems demonstrates the tissue specificity of the DFPM effect (Figure 1F). These marker line analyses suggesting that DFPM targets the primary root meristematic zone led us to further explore how DFPM mediates root growth arrest (described further below).

The *VICTR* Gene Encodes a TIR-NB-LRR Protein

To identify the genetic element(s) in Col-0 producing the *VICTR* phenotype, 100 Col \times *Ler* recombinant inbred lines (RILs) (Clarke et al., 1995) that have been genotyped using microarrays (Singer et al., 2006) were screened for the *VICTR* phenotype (see Supplemental Table 2 online). Quantitative trait locus (QTL) analyses of the phenotypic scores and available genetic map information for these RILs suggested that a single locus in Col-0 positioned on the lower arm of chromosome 5 might determine DFPM-induced root arrest (Figure 2A).

F1 seedlings of Col-0 crosses to *Ler* produced the Col-0 *VICTR* phenotype upon DFPM treatment, indicating that heterozygous expression of the *VICTR^{Col}* allele is sufficient to confer the DFPM response in the *Ler* background. Consistent with QTL analyses of the Col-0 \times *Ler* RILs, F2 seedlings of a Col-0 cross to *Ler* segregated at a ratio of 3:1 (P value of χ^2 test is 0.665, $n = 178$), indicating that a single locus mediates the *VICTR* phenotype. Using these segregating *VICTR* F2 plants, map-based cloning narrowed down the candidate *VICTR* locus to a 100-kb region (Figures 2A and 2B). Since *VICTR* is a natural variant present in Col-0, any polymorphic gene within the target region could encode *VICTR*. Because *VICTR^{Col}* was necessary and sufficient for the DFPM response and was hypothesized to represent an active allele, T-DNA insertion mutants of genes located within the target region in Col-0 were examined. Among the T-DNA lines tested, only T-DNA insertion lines in gene At5g46520 displayed complete insensitivity in DFPM-mediated root growth arrest (Figures 2C and 2D). Five independent T-DNA insertion mutants in the Col-0 At5g46520 gene showed loss of DFPM-triggered root arrest.

DFPM inhibits primary root growth in Col-0 but not in the *vict1* mutants. To determine how DFPM mediates this effect, confocal images of Col-0, *vict1-1*, and *vict1-2* primary roots were analyzed (see Supplemental Figure 3 online). While the quiescent center cells and cortical stem cells appeared unaffected by 24 h of DFPM treatment in all three genotypes, the division zone of the

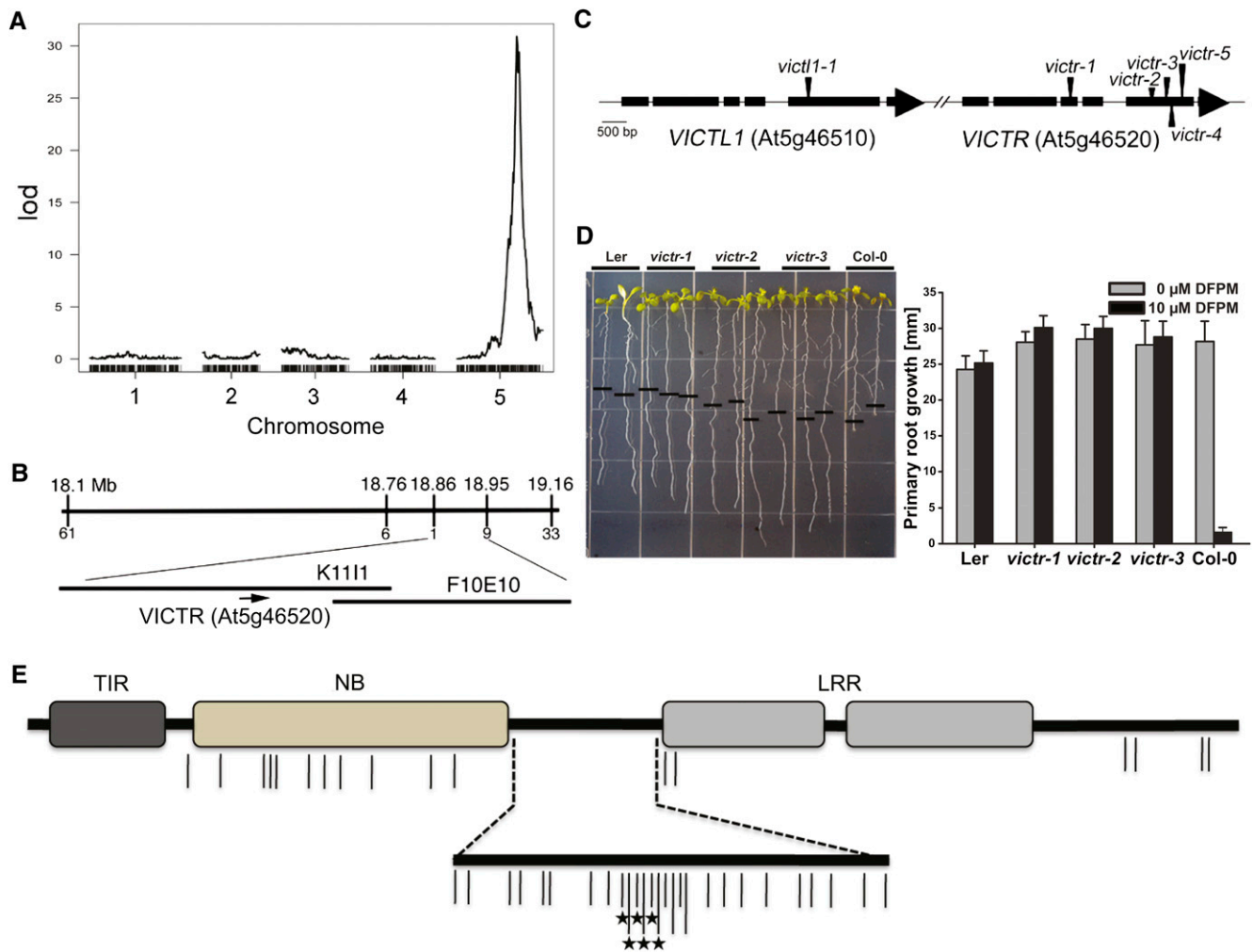


Figure 2. Identification of the Natural Variation *VICTR* Locus.

(A) QTL analyses using the 100 Col \times Ler RILs identified a single locus on chromosome 5 as a main element that triggers the *VICTR* phenotype in Col-0. lod, logarithm of odds.

(B) Map-based cloning using F2 segregants of Col-0 crosses to Ler narrowed down the natural mutation *VICTR*^{Col} within a 100-kb region.

(C) Gene structure of *VICTR*^{Col} and *VICTL1* and the locations of T-DNA insertion mutants.

(D) T-DNA insertion mutants of *VICTR*^{Col} showed complete resistance to DFPM in root growth assays. The black horizontal bars mark the starting position of roots when DFPM was applied. Error bars mean \pm SD ($n = 3$ with 10 plants each).

(E) Protein motif structure of VICTR. Amino acid sequence comparison deduced from the cDNAs of Col-0, Bay-0, and Kin-0 identified multiple Col-0-specific amino acid polymorphisms within the coding region of *VICTR*^{Col}. Vertical lines indicate positions where the Col-0 sequences differ from Bay-0 and Kin-0. It is important to note that Bay-0 and Kin-0 sequences are identical in these positions. Protein sequences other than the TIR, NB, and LRR domains are depicted by black horizontal bars. Asterisks mark amino acid deletions. Most amino acid polymorphisms are found in the NB domain (13 polymorphisms/44 total) and the linker regions between the NB and LRR domains (24 polymorphisms/44 total).

[See online article for color version of this figure.]

DFPM-treated Col-0 primary roots was smaller than that of the *vict-1* and *vict-2* primary roots. To further analyze this phenotype, we quantified the number of meristematic cells in the division zones of primary roots (see Supplemental Figure 3 online). Our data indicate that when treated with DFPM for 24 h, Col-0 primary roots show a reduced number of meristem cells in the division zone of the primary root compared with *vict-1* and *vict-2*. This shorter division zone and the reduced number of meristematic cells are consistent with the inhibition of primary

root growth first observable after 24 h of DFPM treatment in Col-0 wild type and may represent the initial phase of DFPM-induced growth inhibition.

The most similar gene to *VICTR*, *VICTR Like1* (*VICTL1*; At5g46510), is located in tandem upstream of *VICTR* (Figure 2C; see Supplemental Figure 4B and Supplemental Data Set 1 online). A T-DNA mutant *victl1-1* was not resistant to DFPM treatment in the root growth arrest response (see Supplemental Figure 4C online). This suggests that the *VICTR*^{Col} (At5g46520)

gene is required for the chemical DFPM response targeting primary root meristem activity. Chemical genetics can provide an approach for identifying phenotypes in potentially redundant signal transduction genes via small molecule targeting of specific proteins (Park et al., 2009).

VICTR is predicted to encode a previously uncharacterized member of the NB-LRR family with a TIR motif (TIR-NB-LRR) at the N terminus (Figure 2E). TIR-NB-LRR family members can function as immune signaling proteins encoded by *R* genes responding to specific pathogen effectors in plants (Belkhadir et al., 2004; Chisholm et al., 2006; Jones and Dangl, 2006; Shen and Schulze-Lefert, 2007; Caplan et al., 2008). Compared with characterized *R* proteins, the predicted *VICTR*^{Col} protein shows high sequence similarity to that of At1g31540 (64.9% amino acid identity) (Katoch et al., 2002; Thompson et al., 2003; Raghava and Barton, 2006), the Col-0 allele of *RAC1* from accession Ksk-1, which mediates *PAD4*-independent resistance to *Albugo candida* (Borhan et al., 2004). *VICTR*^{Col} is in the same cluster of *R* genes as *RPS6* (At5g46470; see Supplemental Figure 4B online) that specifies resistance to the *Pseudomonas syringae* effector HopA1 (Kim et al., 2009).

To determine whether *VICTR*^{Col} contains unique polymorphism(s) that define the Col-0 sensitivity to DFPM, *VICTR* cDNA sequences from other accessions were reverse transcribed and compared with *VICTR*^{Col}. The *VICTR* gene is highly diverged and possibly absent in *Ler* (Ziolkowski et al., 2009) and also in Wassilewskija-0 (*Ws*-0) based on PCR analysis (see Supplemental Figure 4E online). Comparison of the deduced amino acid sequences in the *VICTR*-containing ecotypes, Bay-0 and Kin-0, shows that *VICTR*^{Col} has multiple unique amino acid polymorphisms centered in the NB domain and the linker region between the NB and LRR domains (Figure 2E; see Supplemental Figure 5A and Supplemental Data Set 2 online). The promoter sequences of the *VICTR* genes are highly conserved (see Supplemental Figure 5B and Supplemental Data Set 2 online).

***VICTR* Expression in DFPM-Insensitive Accessions Generates Col DFPM Responses**

To further establish whether DFPM-induced primary root growth inhibition in Col-0 is dependent on polymorphisms present in the coding region of *VICTR*^{Col}, the *VICTR*^{Col} gene expressed under the control of its natural Col-0 promoter was introduced into accessions insensitive to DFPM: *Ler*, C24, and Bay-0. The introduction of *VICTR*^{Col} was sufficient to generate the DFPM response in primary roots of *Ler*, C24, and Bay-0, demonstrating that *VICTR*^{Col} is the only missing component required for the DFPM-induced primary root growth arrest in these accessions (Figure 3A). As reported for other *R* proteins, ectopic 35S:*VICTR*^{Col} expression in the Col-0 background caused stunted plant growth (see Supplemental Figure 1D online).

***VICTR* Expression Is Increased in the Root Meristematic Zone in a DFPM- and *VICTR*-Dependent Manner**

Resistance genes are generally expressed ubiquitously and at very low levels in unchallenged plants. Electronic *Arabidopsis*

gene expression resources, including AtGenExpress and eFP Browser indicate that *VICTR* is expressed at a low level in many different tissue types (Schmid et al., 2005; Winter et al., 2007). Interestingly, when treated with DFPM for 24 h, *VICTR* was highly induced (eightfold) in the Col-0 background (Figure 3B). Bay-0 and C24, which carry a polymorphic *VICTR* gene relative to *VICTR*^{Col} but are not sensitive to DFPM, did not exhibit enhancement of *VICTR* expression in response to DFPM treatment (Figure 3B). More detailed analyses of *VICTR*^{Col} promoter driven-*GUS* (for β -glucuronidase) reporter and yellow fluorescent protein (*YFP*) reporter lines showed dramatic DFPM-enhanced expression of the *VICTR* gene in the root meristematic zone (Figures 3C and 3D). These results suggest that the DFPM-induced root growth arrest may be caused by differential spatial upregulation of *VICTR* expression in the primary root tip region.

Notably, induction of the *VICTR* gene by DFPM treatment requires functional *VICTR*^{Col} because DFPM could not induce the *VICTR*^{Col} promoter in the *victr-1* mutant (Figure 3D, middle panels). On the other hand, the promoter of *VICTR*^{Bay}, whose sequence is highly similar to that of *VICTR*^{Col} (see Supplemental Figure 5B and Supplemental Data Set 2 online), activated YFP expression by DFPM treatment when introduced into the Col-0 wild type (Figure 3D, bottom panels). Altogether, these results suggest that functional *VICTR* mediates DFPM-induced positive feedback regulation of *VICTR* expression and that amino acid polymorphism(s) in *VICTR*^{Col} are responsible for the *VICTR* phenotype. Consistent with this, Bay-0 expressing *VICTR*^{Col} under the *VICTR*^{Col} promoter exhibited DFPM-mediated root growth arrest (Figure 3A) and also increased *VICTR* expression upon DFPM treatment (Figure 3B). Such positive feedback regulation has been observed for *R* genes and is part of the resistance response induced by corresponding avirulent pathogens (Zhang and Gassmann, 2007).

***VICTR* Requires Effector-Triggered Immune Signaling Components for the DFPM Response**

The finding that *VICTR* encodes a TIR-NB-LRR family R-like protein and previous indications that DFPM induces defense-related gene expression (Kim et al., 2011) raise the hypothesis that pathogen-triggered biotic stress signaling and/or salicylic acid (SA) signaling is responsible for generation of the *VICTR* root growth arrest phenotype. To test this hypothesis and to identify additional genetic components of the DFPM-mediated signaling pathway, pathogen mutants in Col-0 were analyzed to determine whether they exhibit altered root growth responses to DFPM. Among the mutants analyzed, *eds1-2* (Bartsch et al., 2006), *eds1-23*, and *pad4-1* (Glazebrook et al., 1997) mutations disrupted the DFPM-induced root growth arrest, as did the *eds1-2 pad4-1* double mutant (Figure 4A; see Supplemental Figure 4A online). No DFPM resistance was observed in *eds5-1* and *eds16-1*.

EDS1 and PAD4 are also required for DFPM inhibition of ABA-induced stomatal closure (Kim et al., 2011). Therefore, *victr-1* and *victr-2* mutants were analyzed for the ability of DFPM to impair ABA-induced stomatal closing in genotype blind assays. Both *victr-1* and *victr-2* plants showed impairment in DFPM inhibition of ABA-induced stomatal closing (Figure 4B).

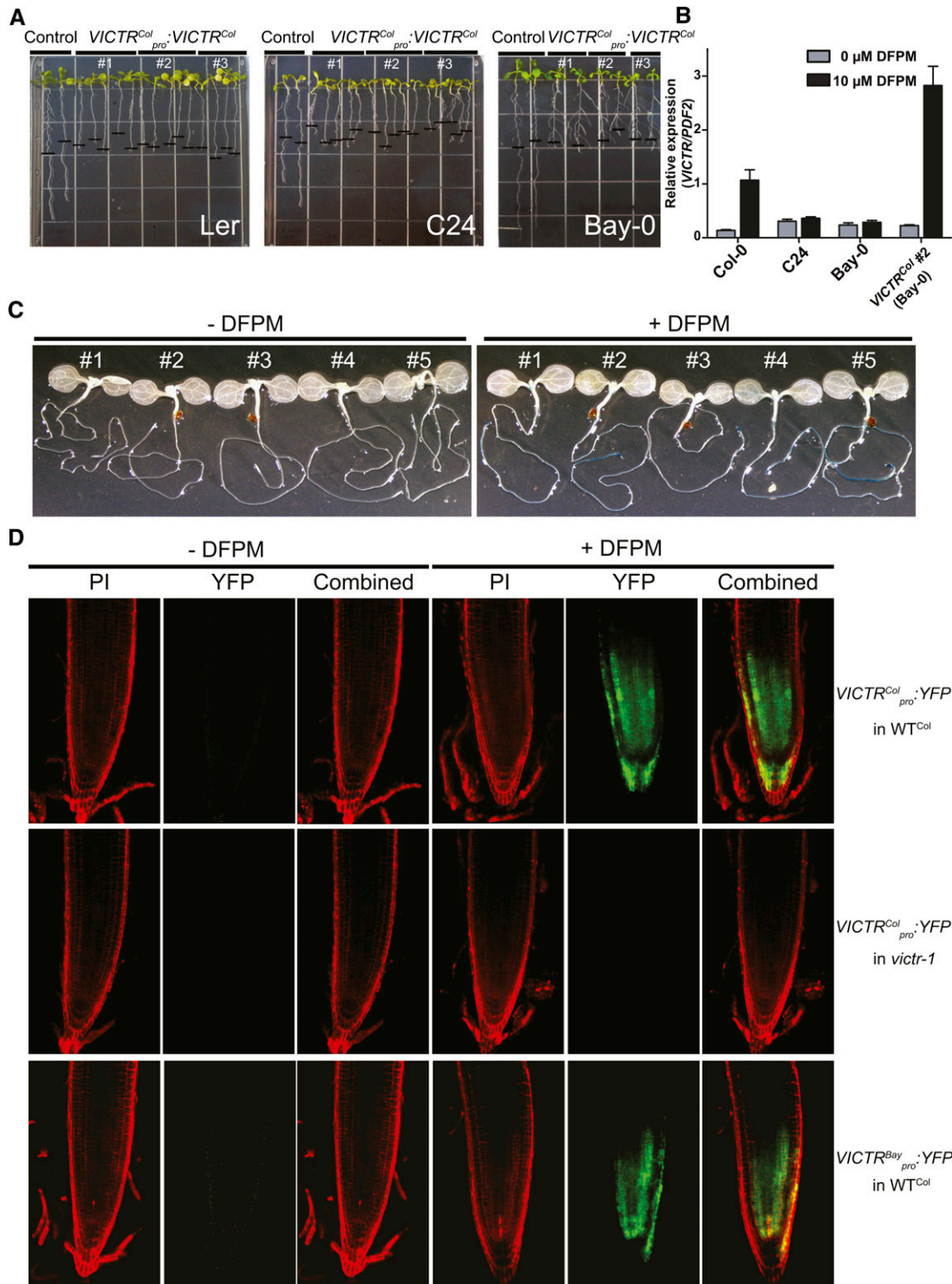


Figure 3. *VICTR^{Col}* Expression Is Sufficient for Generation of the DFPM-Induced Root Meristem Arrest in the DFPM-Resistant Ecotypes Ler, C24, and Bay-0.

(A) Expression of the *VICTR^{Col}* gene under the control of the *VICTR^{Col}* promoter in Ler (left panel), C24 (middle), and Bay-0 (right) reproduced the Col-0 phenotype in response to DFPM. Three independent transgenic lines are shown together with a control transgenic line transformed with empty vector. The black horizontal bars mark the starting position of roots when DFPM was applied.

VICTR Subcellular Localization in Transiently Transformed Cells

To investigate the subcellular localization of VICTR, YFP or GFP fluorophores were fused to either its N or C terminus. All constructs showed that VICTR^{Col} localized to the nucleus with localization also in the cytoplasm as indicated by faint fluorescence in transient onion (*Allium cepa*) epidermis expression assays (see Supplemental Figure 4D online). *Arabidopsis* TIR-NB-LRR proteins, such as RPS4 and RPS6, also display nucleocytoplasmic distributions (Wirthmueller et al., 2007; Kim et al., 2009). In transient *Agrobacterium tumefaciens*-mediated overexpression and immunological detection of the VICTR constructs in *Nicotiana benthamiana* plants, VICTR fusion protein levels were low but detectable based on GFP fluorescence and immunoblots (Figure 5). In *N. benthamiana* expression analyses, we coexpressed red fluorescent protein (RFP) constructs, allowing us to clearly identify transformed cells, visualize nuclei, and perform colocalization analyses. The GFP-VICTR fusion protein was preferentially nuclear localized, and GFP-VICTR fluorescence merged with nuclear RFP (Figure 5A). Although >70% of cells showed RFP expression, GFP-VICTR was detected in only 15 to 20% of transformed cells. Immunoblot analyses identified GFP-VICTR fusions at the expected size (~160 kD), suggesting that the detected fluorescence is not due to either GFP alone or GFP fused to truncated VICTR (Figure 5B).

VICTR Resides in Protein Complexes with Nuclear EDS1 and PAD4

The requirement for EDS1 and PAD4 in DFPM-dependent root inhibition prompted us to investigate in vivo protein complex associations of VICTR with these proteins. Recent studies have shown that the TIR-NB-LRR resistance proteins RPS4 and RPS6 coreside in protein complexes with EDS1 (Bhattacharjee et al., 2011; Heidrich et al., 2011). Pathogen effectors that might signal VICTR-dependent primary root growth arrest are presently not known and effectors that cause root growth arrest have not yet been determined. Such putative effectors may also redundantly use the tandem repeat homolog VICTL1. Identification of molecular interactors of VICTR is relevant toward understanding VICTR protein functions. Bimolecular fluorescence complementation (BiFC), an efficient tool to study in vivo protein-protein interactions, can be used to identify molecular complexes of key innate immunity components (Bhattacharjee et al., 2011). An inherent feature of this assay is its irreversibility, allowing capture of transient interactions. Confocal microscopy analysis of transiently expressed BiFC fusion combinations of VICTR with PAD4 or EDS1 in

N. benthamiana cells suggested nuclear complexes of VICTR with these two proteins (Figure 6). VICTR did not show associations with the reciprocal BiFC vectors expressing GUS that also accumulated inside nuclei (see Supplemental Figure 6A online). Heterodimers of EDS1-PAD4 display nucleocytoplasmic distributions (Feys et al., 2005). However, our BiFC results cannot distinguish whether VICTR associates with EDS1-PAD4 heterodimer-including complexes or within protein complexes individually with EDS1 or PAD4 proteins, which warrants further investigations. Our results suggest cocomplex formation of a TIR-NB-LRR protein with the EDS1 signaling partner PAD4. This is in marked contrast with the TIR-NB-LRR R proteins RPS4 and RPS6, which did not show an interaction with PAD4 in transient expression assays (Bhattacharjee et al., 2011).

We independently investigated the above results by performing coimmunoprecipitation (co-IP) assays on transiently transformed *N. benthamiana* cells (Figure 7A). N-terminally hemagglutinin (HA) epitope-tagged VICTR (HA-VICTR) was coexpressed either with cMyc-tagged-EDS1, -PAD4 or -GUS. Because VICTR expression was enriched in the nucleus, we isolated purified nuclei from the infiltrated leaf tissues and performed nuclear co-IP assays. Both EDS1 and PAD4, but not GUS, coimmunoprecipitated with VICTR (Figure 7A and 7C). These results validated the associations of VICTR with EDS1 and PAD4 proteins in nuclei detected by BiFC (Figure 6).

Using a mutated EDS1, eds1^{L262P}, that does not heterodimerize with PAD4 (Rietz et al., 2011), we tested whether VICTR associates with EDS1-PAD4 heterodimers or individually with EDS1. As expected, the eds1^{L262P} mutant showed a strongly diminished interaction with PAD4 in transient *N. benthamiana* BiFC assays (Figure 7B). We then performed co-IP assays on transiently transformed *N. benthamiana* cells (Figure 7C). N-terminally HA epitope-tagged VICTR (HA-VICTR) was coexpressed either with cMyc-tagged PAD4, -EDS1, -eds1^{L262P}, or -GUS. Purified nuclei from the infiltrated leaf tissues were isolated and nuclear co-IP assays performed. EDS1 wild-type, eds1^{L262P}, and PAD4, but not GUS, coimmunoprecipitated with VICTR (Figure 7C), supporting that VICTR can form complexes with EDS1 and PAD4 inside nuclei.

Senescence Associated Gene101 (SAG101) has also been shown to form a protein complex with EDS1 (Feys et al., 2005; Rietz et al., 2011). As eds1-2 and pad4-1 loss-of-function mutants showed a strong DFPM insensitivity, we tested sag101-2 loss-of-function mutants (Feys et al., 2005) for the DFPM-induced root growth arrest response. In contrast with eds1-2, pad4-1, and eds1-2 pad4-1, sag101-2 mutant plants behaved like Col-0 wild-type controls (Figure 8C). Thus, we propose that

Figure 3. (continued).

(B) DFPM-sensitive *Arabidopsis* lines show induction of VICTR expression by DFPM treatment: five biological replicates for Col-0 and Bay-0 and three for C24 and VICTR^{Col} #2 (Bay-0).

(C) VICTR^{Col} promoter-driven GUS reporter lines in Col-0 background showed tissue-specific and DFPM-dependent induction of VICTR gene expression. Five independent transgenic reporter lines are presented.

(D) VICTR^{Col} promoter-driven YFP reporter line confirms the root tip-specific expression of VICTR after DFPM treatment. No induction of the VICTR^{Col} promoter in *victr-1* indicated that VICTR^{Col} is required for the transcriptional DFPM induction of the VICTR^{Col} promoter. The VICTR^{Bay} promoter drove YFP reporter expression similarly to the VICTR^{Col} promoter. WT, the wild type. PI, propidium iodide.

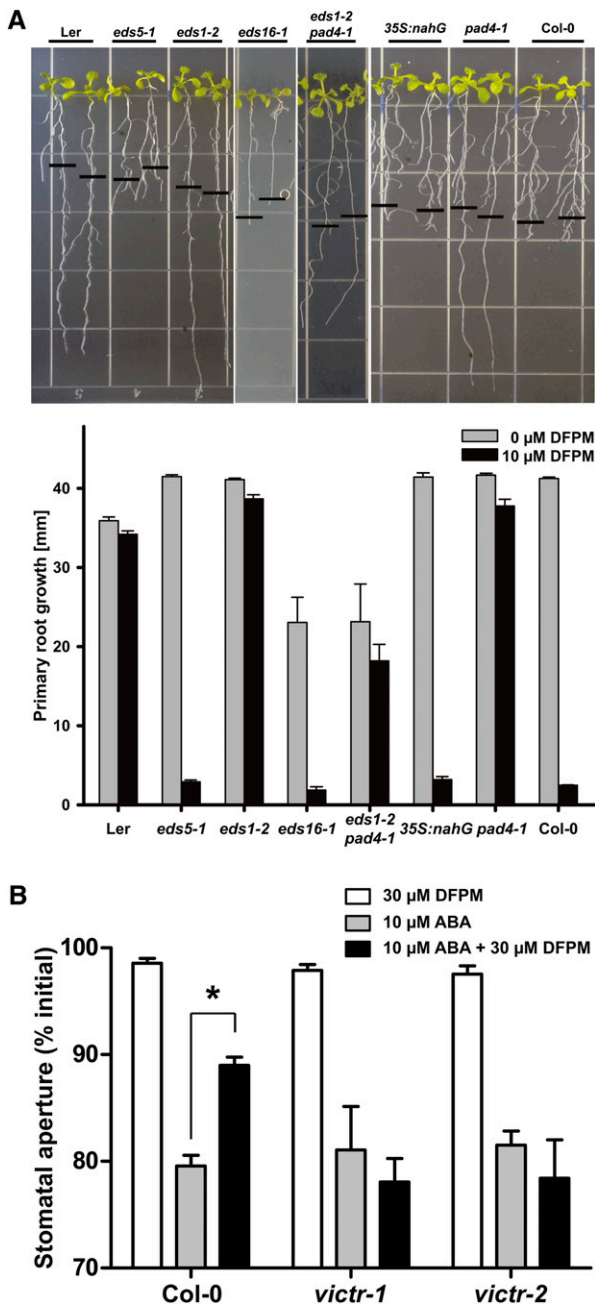


Figure 4. DFPM-Induced Signal Transduction Requires Pathogen Signaling Components.

(A) Chemical signaling by VICTR^{Col} is dependent on EDS1 and PAD4; thus, *eds1-2* and *pad4-1* mutants were insensitive to DFPM, in contrast with *eds5-1* and *35S:nahG*. The black horizontal bars mark the starting position of roots when DFPM was applied. Error bars show \pm SD ($n = 3$ with 10 plants each).

(B) VICTR functions in DFPM inhibition of ABA-induced stomatal closure. Guard cells of *vict-1* and *vict-2* mutants remained sensitive to ABA even in the presence of DFPM. $n = 3$ experiments with 42 to 50 stomata analyzed per condition. Error bars are SE. * $P < 0.01$.

[See online article for color version of this figure.]

DFPM may trigger root growth inhibition by activating an SAG101-independent branch of EDS1-PAD4 signaling.

HSP90 Heat Shock Proteins and Their Cochaperones Are Crucial for DFPM Signaling

The HSP90 chaperones functionally stabilize and maintain R proteins in a signaling-competent state, and their activity is dependent on at least two different cochaperones, RAR1 and SGT1B (Kadota et al., 2010). In root assays, the single mutants *rar1-21* (Tomero et al., 2002) and *sgt1b/eta3* (Gray et al., 2003) exhibited DFPM insensitivity (Figure 8A). Since the *Arabidopsis* genome contains four cytosolic HSP90 isoforms, with three located in close proximity within a 12-kb region on chromosome 5 (Sangster et al., 2007), the effect of the HSP90 inhibitor geldanamycin (GDA) on the DFPM response was analyzed. GDA inhibits cancer cell proliferation by irreversibly binding to the N terminus of HSP90 proteins (Stebbins et al., 1997). A concentration of 5 μ M GDA was sufficient to completely abolish Col-0 specific DFPM root growth inhibition (Figure 8B), consistent

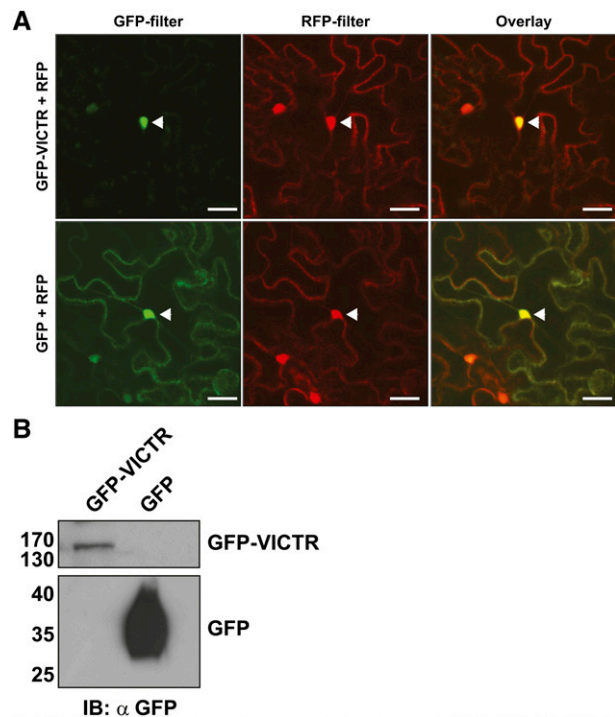


Figure 5. VICTR Localizes to the Nucleus in Plant Cells.

(A) *Agrobacterium* strains expressing GFP-VICTR fusions or GFP alone were coinfiltrated with RFP-expressing strains in *N. benthamiana* leaves. Two days after infiltration, leaf sections were analyzed with a confocal microscope. The left and the middle panels show GFP and RFP fluorescence, respectively. The right panels show an overlap of GFP and RFP fluorescence. Arrowheads point out the nucleus. The assay was repeated with similar localizations. Bars = 20 μ m.

(B) Immunoblots (IB) detecting GFP-VICTR in *N. benthamiana* extracts and showing absence of free GFP or degradation products in GFP-VICTR sample.

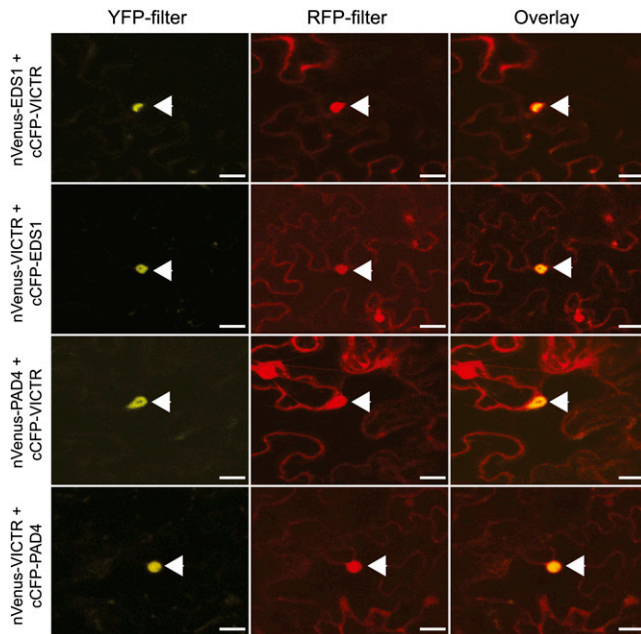


Figure 6. VICTR Associates with Nuclear Pool of EDS1 and PAD4.

Confocal analysis of *N. benthamiana* leaves agroinfiltrated with BiFC vector combinations of VICTR with EDS1 or PAD4. These vector combinations use the N-terminal fragment of an enhanced version of YFP (nVenus) and the C-terminal fragment of CFP (cCFP), which when reconstituted gives yellow fluorescence (Hu and Kerppola, 2003). Localization of indicated molecular complexes is shown by yellow fluorescence. Red fluorescence indicates free RFP. Panels show images with separate YFP, RFP, and an overlap of YFP + RFP fluorescence. Arrowheads indicate the nucleus. The experiment was repeated with identical results ($n = 3$). Bars = 20 μm .

with the observed DFPM resistance of *rar1-21* and *sgt1b/eta3* (Figure 8A). This suggests that HSP90 cooperates with RAR1 and SGT1B to stabilize VICTR as a prerequisite for the DFPM root growth response.

DFPM Response Does Not Require Jasmonic Acid or SA Signaling

The *eds5-1* mutant defective in SA biosynthesis (Rogers and Ausubel, 1997) and a SA-depleted *35S:nahG* transgenic line (Reuber et al., 1998) were not affected in the DFPM-induced root growth response (Figure 4A). With the exception of the resistance signaling components described above, other known pathogen response loci were also not required for the DFPM-induced root growth arrest. These include the NB-LRR genes *RPS2*, *RPM1*, and *RPS4*, immune signaling and response components *NPR1*, *NPR3-NPR4*, *PAD3*, and *PMR4*, and a pathogen-associated molecular pattern (PAMP) receptor, *FLS2*, as well as the jasmonic acid (JA) signaling components *COI1* and *JAI1/JIN1* (Lorenzo et al., 2004; Zhang et al., 2006; Fonseca et al., 2009; Sheard et al., 2010; Fu et al., 2012) (Figure 8C). Although application of exogenous SA also caused root growth inhibition (see Supplemental Figure 7A online), detailed

inspection showed that the SA effect on root growth inhibition is morphologically clearly distinct from the DFPM-induced root growth arrest in several respects. SA blocks general growth of *Arabidopsis* seedlings (Zhang et al., 2003a), including root elongation, lateral root initiation, and root hair formation (see Supplemental Figure 7B online), in contrast with DFPM (e.g., Figure 4A; see Supplemental Figure 2B online). Also, the SA-induced root growth inhibition is not accession specific because the response to SA was equivalent in Col-0 and Ler.

DISCUSSION

We identified genetic natural variation in the *VICTR* locus that produces root growth arrest in response to the small molecule DFPM. We report that DFPM perception and signal transduction requires early components of the plant *R* gene resistance signaling network, including the TIR-NB-LRR protein VICTR^{Col}, EDS1, and PAD4. This response may also involve VICTR stabilization by HSP90 together with RAR1 and SGT1B but operates independently of major defense signaling components in the JA and SA signal transduction pathways. VICTR^{Col} is also required for DFPM-induced inhibition of ABA-induced stomatal closing, further showing that early TIR-NB-LRR signaling rapidly interferes with ABA signal transduction. We further establish in transient protein expression assays that VICTR resides within nuclear protein complexes with EDS1 and PAD4. By contrast, the nucleocytoplasmic TIR-NB-LRR receptors RPS4 and RPS6 were found only in complexes with EDS1 and not PAD4 (Bhattacharjee et al., 2011; Heidrich et al., 2011). Thus, different types of TIR-NB-LRR receptors may operate in distinct resistance signaling complexes containing EDS1 and/or PAD4. Previously, it was shown that the *eds1*^{L262P} mutant, which does not interact with PAD4 (Figure 7B), has defects in basal immunity to virulent pathogens (Rietz et al., 2011). The retention of a co-IP signal between VICTR and *eds1*^{L262P} protein in transient expression assays (Figure 7C) suggests that this mutation may not be crucial for TIR-NB-LRR protein-EDS1 complex formation.

A requirement for VICTR interactors EDS1 and PAD4 in the DFPM-induced response and microarray analyses support the notion that a plant effector-triggered immunity signaling pathway (Glazebrook, 2005; Wiermer et al., 2005; Kim et al., 2011) mediates the DFPM response (Figure 4A). Furthermore, the requirement of *RAR1* and *SGT1B* and HSP90 chaperones suggests that VICTR steady state accumulation and possibly also chaperone-mediated conformational changes are important for DFPM-triggered VICTR signaling (Shirasu, 2009) (Figures 8A and 8B). However, the lack of requirement for other analyzed defense signaling elements, including key components of the SA-signaling and JA-signaling pathways (Lorenzo et al., 2004; Zhang et al., 2006; Fu et al., 2012), suggests that a SA/JA-independent disease signaling network participates in the DFPM-induced root growth arrest (Figures 4A and 8C). Since *PIN1:GFP* and *PIN2:GFP* expression was decreased after 18 h of DFPM treatment, an involvement of auxin cannot be ruled out and warrants further analysis. Auxin binding-specific fluorescence reporters (Brunoud et al., 2012) with a rapid readout may be required to unequivocally resolve this question.

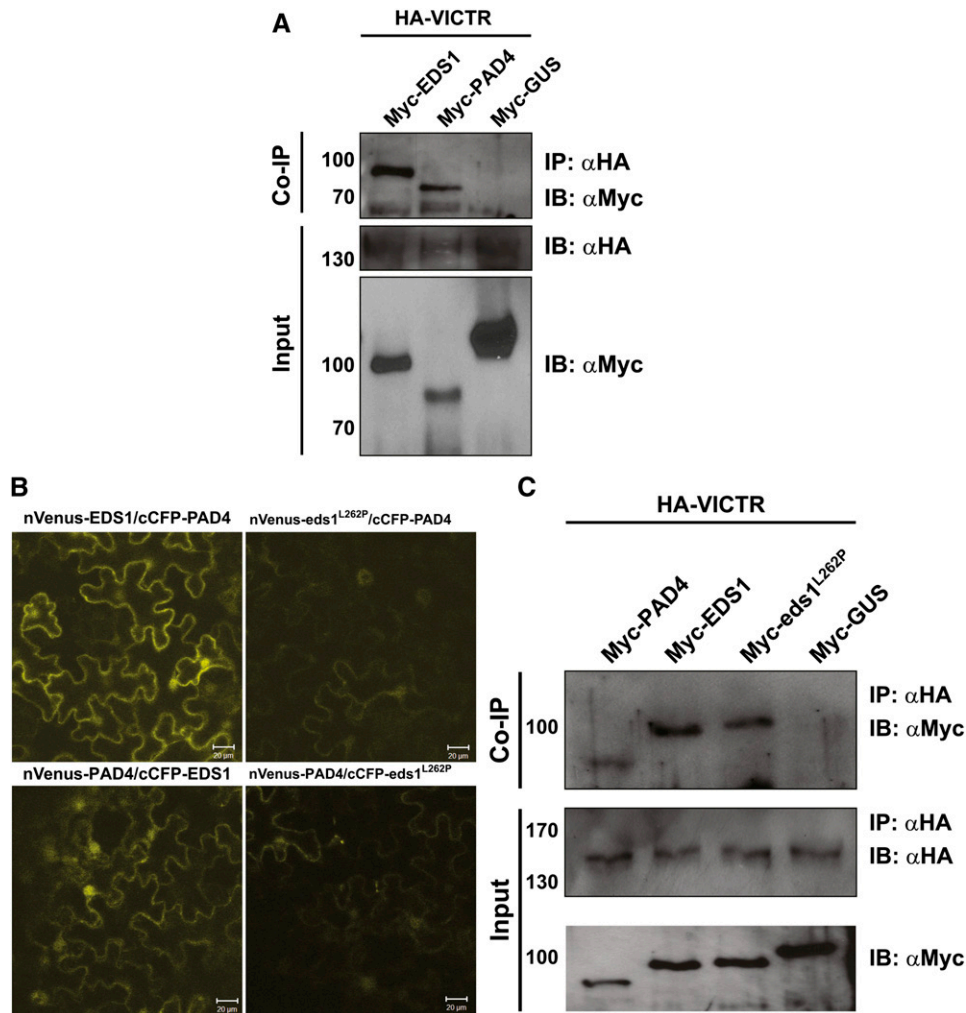


Figure 7. VICTR Associates in Planta with EDS1, PAD4, and eds1^{L262P}.

(A) Myc-tagged EDS1, PAD4, and GUS were transiently coexpressed with HA-VICTR in *N. benthamiana* leaves. Purified nuclear extracts were immunoprecipitated (IP) and immunoblotted (IB) with the indicated antibodies. Top panel shows the pull-down of PAD4 and EDS1, but not GUS, with VICTR. Bottom two panels show input fractions ($n = 3$).

(B) eds1^{L262P} does not strongly interact with PAD4 in BiFC assays. Reciprocal BiFC assays of PAD4 with wild-type EDS1 and eds1^{L262P} were performed by *Agrobacterium*-mediated transient expression in *N. benthamiana*. Reconstituted YFP is indicated by yellow fluorescence. Bar values are indicated.

(C) VICTR interacts with eds1^{L262P}. Co-IP was performed as described above. Top panel is the co-IP of PAD4, EDS1, and eds1^{L262P}, but not GUS, with VICTR. Bottom two panels show the input fractions. HA-VICTR was detected only after immunoprecipitation with anti-HA antibodies. Migration and sizes (in kilodaltons) of molecular mass standards are at the left of the respective immunoblot panels. Each experiment was performed twice with similar results.

DFPM may activate TIR-NB-LRR-mediated signal transduction by mimicking a pathogen effector (Belkadir et al., 2004; Jones and Dangl, 2006; Caplan et al., 2008), analogous to the organophosphate insecticide fenthion that triggers an immune-like response via the kinase Fen and the NB-LRR protein Prf in tomato (*Solanum lycopersicum*; Pedley and Martin, 2003). Activation of effector-triggered immunity can promote infection by necrotrophic pathogens that feed off dead plant tissue (Glazebrook, 2005). Interestingly, certain necrotrophic fungal pathogens secrete small toxin molecules (such as victorin produced by *Cochliobolus victoriae*), which are sensed by NB-LRR

proteins (Sweet and Wolpert, 2007; Lorang et al., 2012). When primary roots are challenged by soil-borne pathogens, localized VICTR responses may limit damage to the root and function in restriction of primary root growth, thereby protecting roots from further infection. Given the homology of VICTR and its tandem gene *VICTL1*, biological responses may be mediated redundantly via either of these two proteins. Chemical genetics provides a powerful approach for identification of redundant signaling genes and their linked phenotypes by protein-specific selective activation, as in the case of the discovery of the redundant PYR1 ABA receptor (Park et al., 2009). Whether VICTR

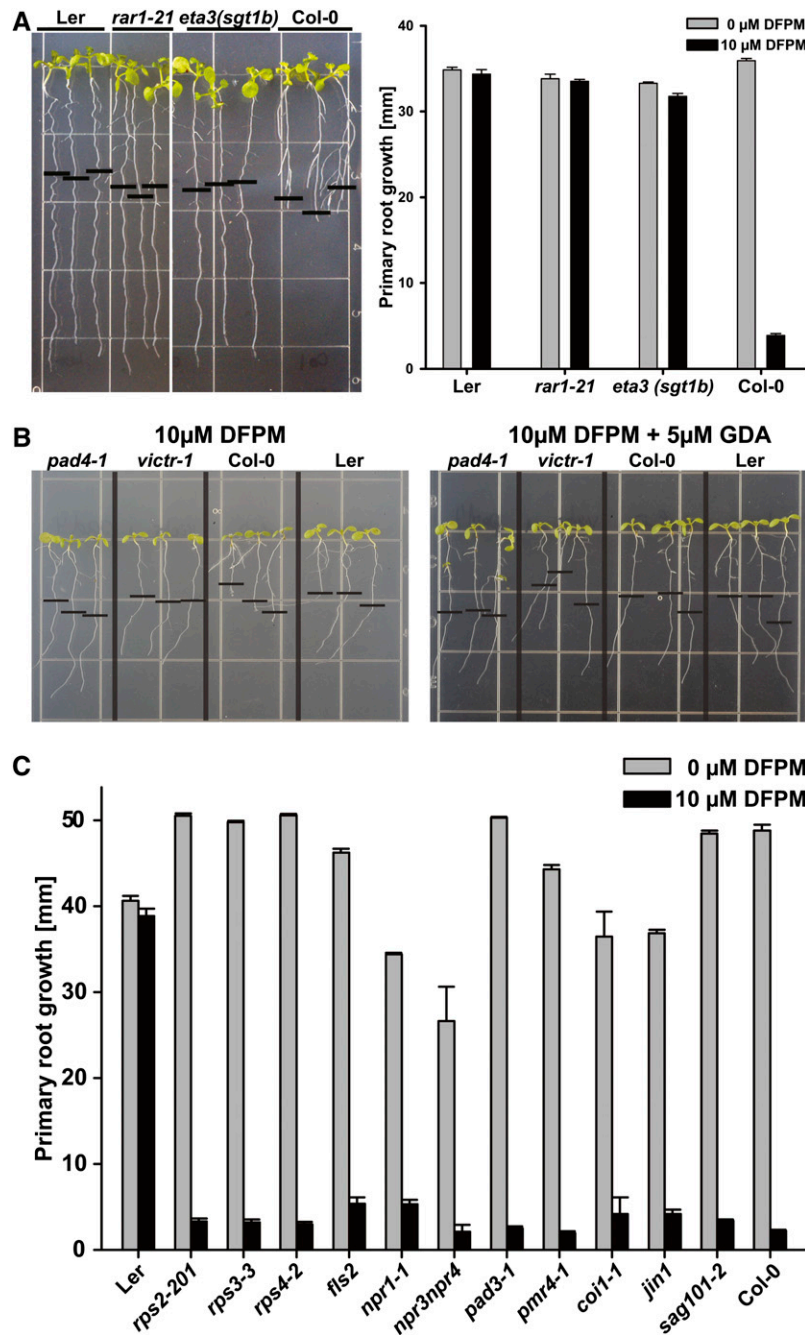


Figure 8. The DFPM-Induced Signal Transduction Relies on HSP90 and Its Cochaperones but Does Not Require SAG101, SA, and JA Signaling Components.

(A) Chemical signaling by *VICTR^{Col}* requires functional HSP90 cochaperones RAR1 and SGT1B.

(B) The DFPM signal was blocked by applying additional 5 μM of the HSP90 inhibitor GDA.

(C) Other signaling and response components known to function in pathogen, SA, and JA signal transduction or other *NB-LRR* genes are not required for the *VICTR* phenotype. All mutants were tested in Col-0 background. Error bars mean \pm sd. Note, some error bars are not visible due to very small sd ($n = 3$ with 10 plants each).

[See online article for color version of this figure.]

and *VICTL1* function in concert in biologically induced root growth arrest will require identification of natural effectors that stimulate this root response in *Arabidopsis*.

DFPM was identified as a small molecule that rapidly inhibits ABA responses (Kim et al., 2011). DFPM interference with ABA signal transduction also required PAD4, EDS1, RAR1, and SGT1B but not SA or JA signal transduction components (Kim et al., 2011). As shown in stomatal movement analyses, DFPM inhibition of ABA-induced stomatal closing is impaired in *vict1* T-DNA insertion mutant stomata (Figure 4B), supporting the previous model that DFPM mediates inhibition of ABA signal transduction via early effector-triggered immune signaling (Kim et al., 2011). A requirement for VICTR in this response is consistent with data sets showing *VICTR* expression in leaves (Schmid et al., 2005; Winter et al., 2007).

TIR-NB-LRR genes mainly function in resistance against pathogens. Retention of nonfunctional *R* gene alleles and a statistically significant increase in the occurrence of *R* gene polymorphisms is hypothesized to be an outcome of fitness tradeoffs in evolving a large array of recognition specificities in a plant population (Tian et al., 2003; Weigel, 2012). An additional consequence of natural variants in *NB-LRR* genes can be environmentally conditioned hybrid necrosis (Bomblies et al., 2007; Alcázar et al., 2009). TIR-NB-LRR-mediated root growth arrest has not been reported previously. Here, we show that DFPM inhibits root growth via *VICTR*^{Col} in an *EDS1/PAD4/RAR1/SGT1B/HSP90*-dependent manner. These data suggest a direct link between *R* gene-related signaling and root growth arrest. DFPM causes a rapid root growth arrest along with a decreased cell division rate in the primary root meristematic zone in Col-0. However, the quiescent center cells and cortical stem cells appear unaffected after 24 h DFPM treatment in both resistant and sensitive genotypes, a time point at which initial root growth inhibition becomes visible. These findings and the DFPM-induced *VICTR* promoter activity in wild-type plants suggest a role for VICTR protein levels in determining this interesting root meristem-localized EDS1- and PAD4-dependent response. As described for delocalized or overexpressed *R* proteins (Zhang et al., 2003b; Yi and Richards, 2007; Kim et al., 2010), ectopic *VICTR* expression also leads to stunted growth phenotypes.

Identification of the small molecule DFPM as a trigger of an effector-triggered immune-related signaling pathway that causes a strong visual and quantifiable primary root growth arrest can provide a powerful tool for further genetic dissection of *R* gene-mediated signaling. This is demonstrated here by the identification of the *VICTR* gene and findings showing association of PAD4 and EDS1 within VICTR protein complexes. Also, genetic variation in this small molecule response in *Arabidopsis* accessions is consistent with the hypothesis that the repertoire of *TIR-NB-LRR* genes provides activation mechanisms to diverse cues and here via a root meristem-targeted response.

METHODS

Chemicals and Plant Materials

DFPM (ID 6015316) was isolated from screening of 9600 compounds in ChemBridge's DIVERSet E library. DFPM (ID 6015316), DFPM-1 (ID

5649754), DFPM-2 (ID 5872683), DFPM-3 (ID 6881095), DFPM-5 (ID 6017927), and DFPM-7 (ID 5143713) were purchased from ChemBridge. Transgenic reporter lines were in the Col-0 background or were crossed into the Col-0 background. *Arabidopsis thaliana* T-DNA lines were obtained from the ABRC (Ohio State University).

Arabidopsis ecotype set CS22660, *vict1-1* (Salk_123918), *vict1-2* (Salk_084068), *vict1-3* (Salk_072727), *vict1-4* (Salk_122941), *vict1-5* (Salk_394_F01), *vict1-1-1* (Salk_097845), *eds1-23* (Salk_057149), and Caroline Dean's 100 Col × *Ler* RILs (CS1899) (Clarke et al., 1995; Singer et al., 2006) were obtained from the ABRC (Ohio State University). The *eds1-23* T-DNA mutant (Salk_057149) has a T-DNA insertion in At3g48090, one of a tandem pair of EDS1 homologs in accession Col-0. Another T-DNA insertion mutant (Salk_071051) in the same gene, denoted *eds1-22*, substantially rescues the growth phenotype of *bon1-1* constitutive resistance plants (Yang and Hua, 2004). *pDR5:GFP*, *pPIN1:PIN1:GFP*, and *pPIN2:PIN2:GFP* were kindly provided by Yunde Zhao (University of California at San Diego). *pSCR:GFP* and *pCyclinB1:GUS* were kindly provided by Jeff Long (Salk Institute) and Jeff Harper (Univ. of Nevada), respectively. Mutants *eds1-2* (Bartsch et al., 2006) and *sag101-2* (Feys et al., 2005), *pad4-1* and *pmr4-1* (Nishimura et al., 2003), *rar1-21* (Tornerio et al., 2002), *eta3/sgt1b* (Gray et al., 2003), *fls2* (Gómez-Gómez and Boller, 2000), *eds5-1* (Rogers and Ausubel, 1997) 35S:*nahG* line (Reuber et al., 1998), and *npr3-2npr4-2* (Fu et al., 2012) were kindly provided by Jane Glazebrook (University of Minnesota), Jeff Dangl (University of North Carolina), William Gray (University of Minnesota), Shauna Somerville (University of California at Berkeley), Sheng Yang He (University of Michigan), Mary Wildermuth (University of California at Berkeley), and Xin Li (University of British Columbia, Canada), respectively.

Root Growth Assays

Sterilized *Arabidopsis* seeds were germinated on general growth medium (1% Suc, 0.5× Murashige and Skoog [MS] salts, 0.05% MES, and 0.8% plant agar, pH 5.8) after 2 d of stratification and vertically grown for 10 d before transfer to new plates containing the indicated chemicals. After transfer onto new plates, the end of each root was marked as a starting point, and root growth arrest was monitored after 6 d. Root morphology and GUS staining were examined by differential interference contrast microscopy (Leica DM5000B), and fluorescence reporter lines were analyzed by confocal microscopy (Nikon TE2000U) with propidium iodide staining.

Confocal Microscopy

Col-0, PIN1:GFP, and PIN2:GFP plants were grown vertically in half-strength MS medium containing 1% Suc for 5 d and transferred to 10 μM DFPM half-strength MS medium. At the indicated time, primary roots were stained with propidium iodide and observed using a Zeiss LSM 710 confocal microscope with spectral settings for excitation at 488 nm/emission at 493 to 555 nm for the GFP signal and excitation 514 nm and emission at 596 to 719 nm for propidium iodide. A constant gain value was used for each genotype. For root meristem cell quantification, Col-0, *vict1-1*, and *vict1-2* plants were prepared as described above. Meristem cells in the division zone were counted using Image J (Schneider et al., 2012). A single file of cortex cells was analyzed in all roots. The division zone was defined as the region made up of isodiametric cells between the quiescent center up to the cell, which was twice the length of the cell immediately before it (González-García et al., 2011). analysis of variance and Tukey test statistical analyses were conducted using the Origin-Pro version 8.6 package. Ten seedlings per genotype and treatment were analyzed.

QTL Analyses and *VICTR* Cloning

For initial mapping and QTL analyses, the DFPM-induced *VICTR* phenotype was scored on the 100 Col \times Ler RILs. QTL analyses were performed using QTL package (version 1.11-12) that uses R software (version 2.81) based on the QTL package manual (Broman et al., 2003). Parameters used for LOD estimation were step = 1 and error probability = 0.01. Haldane map function was used as a mapping algorithm. Genotyping information of each Col \times Ler RILs was retrieved from the microarray-based physical genomic mapping data set (Singer et al., 2006).

For marker-based cloning of the *VICTR^{Col}* locus, the recessive *Ler* root development phenotype was screened from a mapping population of ~2000 F2 plants of Col crosses to *Ler*. The *VICTR^{Col}* locus was mapped to an ~5-centimorgan interval on the lower arm of chromosome 5 based on linkage to PCR-based markers 18.1 Mb (5'-GTCGTAGAAGTAGCAGCTTGACGAAGT-3'/5'-TCTCAATCCAATGTTTCAGGTGACACACT-3') and 19.1 Mb (5'-GAA-TCTCTAACGATGCTAACACAAGGA-3'/5'-CTGCAATCACAGTTAAGTCAT-GAACT-3'). Within the 100-kb region defined by markers 18.86 and 18.95 Mb, 21 T-DNA insertion lines targeting 14 genes among 18 predicted genes (*At5g46490* to *At5g46650*) were analyzed for the root *VICTR* phenotype.

Deletion of *VICTR* in certain ecotypes (see Supplemental Figure 4 online) was examined by PCR amplification of genomic DNA templates using LA Taq and Ex Taq polymerases (Takara Bio). Control primers are 5'-ATGGTTGCGATACCCAATATTAAGA-3' and 5'-CTAAAGGATCT-CTCCTTCTCAAGATCGT-3'. Internal primers are 5'-CGGGTAGA-AATATTGTACGCTCACAGT-3' and 5'-CCAAATGGTTGAGAGTCAG-ATGTTT-3'. Note that internal primers anneal to both *VICTR* and *VICTL1*. External primers are 5'-GGACGCTTTGTTCCAGCTTGTG-GGGCATTAAATCGAG-3' and 5'-CACTTCGTAGGGCGTTGGGGCA-GACATTGCCCTTCTC-3'.

Transgenic Studies

To generate *VICTR* promoter-driven reporter lines, a 2.5-kb fragment from the start codon of Col-0 and Bay-0 was PCR amplified from genomic DNA using primers (5'-GGGGACAAGTTTGTACAAAAAAGCAGGCTGAGAACCAGTACACAATGGCAGGTAAG-3'/5'-GGGGACCACTTTGTACAAGAAAGCTGGG-TAAGAAGCCATAGAGAGAGTTAGAAGGAGGA-3') and cloned into pBGGUS and pHGY (vector plasmids were kindly provided by Taku Demura from RIKEN) (Kubo et al., 2005). The *VICTR^{Col}* gene was PCR amplified using primers 5'-GGGGACAAGTTTGTACAAAAAAGCAGGCTGCCCTGTGGTA-TCTGGTAATCAAATCTGT-3'/5'-GGGGACCACTTTGTACAAGAAAGC-TGGGTGGCTACAAAGCAAGTCAGTCGTTCTGTTG-3'. The *VICTR^{Col}* coding region for the 35S promoter driven transgenic line was PCR amplified using primers 5'-GGGGACAAGTTTGTACAAAAAAGCAGGCTTCTCTCTCTAA-CTCTCTCTATGGCTTC-3'/5'-GGGGACCACTTTGTACAAGAAAGCTGGG-TCTCATATGAAGTGGTGTAGCTGCAAAAG-3'. For recapitulation of the Col-0 *VICTR* phenotype in *Ler* and C24, the *VICTR^{Col}* gene including the promoter and coding region was inserted into pHGY. For generation of 35S promoter-driven *VICTR^{Col}* transgenic lines, the *VICTR^{Col}* coding region, including introns, was cloned into pH35GS. Transformed lines with empty vector were used as controls for phenotypic analyses.

For subcellular localization analysis in onion (*Allium cepa*) epidermal cells (see Supplemental Figure 4D online), full-length *VICTR^{Col}* cDNA was inserted into pH35GY and pH35YG to construct plasmids encoding *VICTR*-YFP and YFP-*VICTR*, respectively. Transient expression by biolistic bombardment (using PDS-1000/He; Bio-Rad) was performed in onion epidermal cells.

Localization and Immunodetection of *VICTR* in *Nicotiana benthamiana* Cells

VICTR cDNA in the entry vector (pENTR-TOPO-*VICTR*) was transferred via Clonase LR recombination system (Invitrogen) into the Gateway-

compatible destination vector pMDC43 (Curtis and Grossniklaus, 2003), resulting in a *GFP-VICTR* expression vector. The RFP vector used in colocalization analysis was described earlier (Bhattacharjee et al., 2011). *N. benthamiana* leaves were infiltrated with the indicated *Agrobacterium tumefaciens* strains at an OD₆₀₀ of 0.3 for each strain. Two days after infiltration, tissue sections from the infiltrated patches were analyzed by a two-photon equipped Zeiss confocal microscope. Three 7-mm-diameter leaf punches were excised from the infiltrated tissues and ground in 100 μ L of 8 M urea and subjected to immunoblotting with anti-GFP antibodies (Sigma-Aldrich).

BiFC Assays

The pENTR-TOPO-*VICTR* clone was recombined into the Gateway-compatible BiFC vectors pMDC-nVenus or pMDC-cCFF (Bhattacharjee et al., 2011) using the Clonase LR recombination system. BiFC vectors for EDS1, PAD4, and GUS expression were used as in previous studies (Bhattacharjee et al., 2011). Agroinfiltration and confocal microscopy analysis were performed as indicated earlier. For fusion protein detection, three 7-mm-diameter leaf discs were excised from the infiltrated patches, ground in 8 M urea and analyzed by immunoblotting using anti-GFP antibodies (Santa Cruz Biotechnology).

Coimmunoprecipitation Analyses

HA-tagged *VICTR* was generated using pENTR-TOPO-*VICTR* and the destination vector HA-pBA (Kim et al., 2010). Myc-tagged EDS1, PAD4, and GUS have been used before (Bhattacharjee et al., 2011). The eds1^{L262P} mutant described by Rietz et al. (2011) was generated by overlap PCR using the primers 5'-TTCCTGAGCTAAGTCTTATA-3' and 5'-GCTCAGGGAAACTAGAAAGGT-3' and replacing the wild-type fragment in the entry clone of EDS1. Myc-eds1^{L262P} was generated by Clonase recombining the entry clone into the Myc-pBA binary vector. *Agrobacterium*-infiltrated *N. benthamiana* leaves were processed for nuclear extracts as described by Palma et al. (2007). The resulting nuclear lysates were centrifuged at 14,000g for 10 min to remove nuclear debris. Immunoprecipitation was performed as published before (Bhattacharjee et al., 2011). The immunoprecipitates and the input fractions were analyzed with anti-HA (Roche) or anti-Myc (Santa Cruz Biotechnology) antibodies.

Quantitative Real-Time RT-PCR

Col-0, C24, Bay-0, and one line of Bay-0 expressing *VICTR^{Col-0}* were grown in half-strength MS media for 14 d and were transferred to half-strength MS containing 10 μ M DFP. After 24 h of DFP treatment, total RNA was extracted, and real-time RT-PCR was performed to quantify the transcript levels of *VICTR*. Primers were designed with QuantPrime (Arvidsson et al., 2008): *VICTR*-qRT2-F, 5'-AGAGACCGGTTTCATCAG-CAGAG-3'; *VICTR*-qRT2-R, 5'-CCATATTGCCCTTCTCGGCTTGAG-3'. Amplified samples were normalized against *PDF2* levels: *PDF2_F*, 5'-TAACGTGGCCAAATGATGC-3'; *PDF2_R*, 5'-GTTCTCCACAACCGCT-TGGT-3'.

Stomatal aperture measurements were performed as described before (Kim et al., 2011; Hubbard et al., 2012). Student's *t* tests were performed for *n* = 3 independent experiments with 42 to 50 stomata analyzed for each condition.

Accession Numbers

Sequence data from this article can be found in the Arabidopsis Genome Initiative database under the following accession numbers: *VICTR*, At5g46520; *VICTL1*, At5g46510; EDS1, At3g48090; and PAD4, AT3G52430.

Supplemental Data

The following materials are available in the online version of this article.

Supplemental Figure 1. Functional Characterization of Modified DFPM Structures and *35S:VICTR^{Col}* Ectopic Expression Caused Stunted Growth.

Supplemental Figure 2. Gene Expression and Morphological Changes of DFPM-Treated Seedlings.

Supplemental Figure 3. DFPM Reduces the Number of Meristem Cells in the Wild Type, but Not in *vict1* Mutant Alleles.

Supplemental Figure 4. Characterization of *eds1-23* T-DNA Insertion Line and *vict1-1*, Subcellular Localization of VICTR, and VICTR Deletion in Other Accessions.

Supplemental Figure 5. VICTR Gene Sequence Comparison of Col-0 with Bay-0 and Kin-0.

Supplemental Figure 6. VICTR Does Not Associate with GUS.

Supplemental Figure 7. Root Growth Inhibition by Salicylic Acid Differs from the DFPM-Induced Primary Root Growth Arrest Response.

Supplemental Table 1. List of *Arabidopsis* Accessions That Did Not Produce the Root Developmental Arrest in Response to DFPM Treatment.

Supplemental Table 2. DFPM-Induced Root Growth Arrest VICTR Phenotype in 100 Col × *Ler* Recombinant Inbred Lines.

Supplemental Data Set 1. Text File of the Alignment Used to Generate the Phylogenetic Tree Shown in Supplemental Figure 4B.

Supplemental Data Set 2. Text File of the Alignment in Supplemental Figure 5.

ACKNOWLEDGMENTS

We thank Chris Somerville (University of California at Berkeley) for providing access to the chemical library of 9600 compounds, Jeff Dangl for providing *rar1-21* seeds, and Amber Ries [University of California at San Diego (UCSD)] for independent blinded stomatal movement analyses. We thank Rosangela Sozzani (University of Pavia), Yunde Zhao, Sangho Jeong, Aurelien Boisson-Dernier, Noriyuki Nishimura and Carolyn Rasmussen at UCSD for comments on the article and helpful discussions. This research was supported by the National Institutes of Health (R01GM060396; J.I.S.), the National Science Foundation (MCB0918220, J.I.S.; IOS1121114, W.G.), and the Max-Planck Society and Deutsche Forschungsgemeinschaft 'SFB 670' (J.E.P) grants. Root growth analyses were in part funded by a grant from the Division of Chemical Sciences, Geosciences, and Biosciences, Office of Basic Energy Sciences of the U.S. Department of Energy (DE-FG02-03ER15449; J.I.S.) and in part by the National Research Foundation of Korea funded by the Ministry of Education, Science and Technology (2012-0002781 and 2012-041653) to T.-H.K. H.-H.K. was funded by the Human Frontier Science Program and the Alexander von Humboldt Foundation.

AUTHOR CONTRIBUTIONS

T.-H.K. and J.I.S. designed the experiments. T.-H.K. performed most of the experiments. S.B., H.-H.K., W.G., and J.I.S. designed BiFC and co-IP experiments. S.B. and H.-H.K. prepared constructs and S.B. conducted BiFC and co-IP experiments. H.-H.K. worked on GDA/DFPM interference

and distributed material. A.L. conducted stomatal movement analyses. T.-H.K., F.H., H.-H.K., W.G., J.E.P., and J.I.S. analyzed the data. C.E. analyzed meristematic cell division, J.P. contributed quantitative PCR, *pPIN:PIN:GFP* results, and repeated *pDR5:GFP* data. S.B., H.-H.K., W.G., and J.E.P. contributed to the *eds1^{L262P}* experiment. T.H. assisted with the VICTR cloning. T.-H.K., H.-H.K., and J.I.S. wrote the article with input from other coauthors.

Received November 8, 2012; revised November 8, 2012; accepted December 13, 2012; published December 28, 2012.

REFERENCES

- Alcázar, R., García, A.V., Parker, J.E., and Reymond, M. (2009). Incremental steps toward incompatibility revealed by *Arabidopsis* epistatic interactions modulating salicylic acid pathway activation. *Proc. Natl. Acad. Sci. USA* **106**: 334–339.
- Armstrong, J.I., Yuan, S., Dale, J.M., Tanner, V.N., and Theologis, A. (2004). Identification of inhibitors of auxin transcriptional activation by means of chemical genetics in *Arabidopsis*. *Proc. Natl. Acad. Sci. USA* **101**: 14978–14983.
- Arvidsson, S., Kwasniewski, M., Riano-Pachon, D.M., and Mueller-Roeber, B. (2008). QuantPrime—A flexible tool for reliable high-throughput primer design for quantitative PCR. *BMC Bioinformatics* **9**: 465.
- Bartsch, M., Gobbato, E., Bednarek, P., Debey, S., Schultze, J.L., Bautor, J., and Parker, J.E. (2006). Salicylic acid-independent ENHANCED DISEASE SUSCEPTIBILITY1 signaling in *Arabidopsis* immunity and cell death is regulated by the monooxygenase FMO1 and the Nudix hydrolase NUDT7. *Plant Cell* **18**: 1038–1051.
- Belkhadir, Y., Subramaniam, R., and Dangl, J.L. (2004). Plant disease resistance protein signaling: NBS-LRR proteins and their partners. *Curr. Opin. Plant Biol.* **7**: 391–399.
- Bhattacharjee, S., Halane, M.K., Kim, S.H., and Gassmann, W. (2011). Pathogen effectors target *Arabidopsis* EDS1 and alter its interactions with immune regulators. *Science* **334**: 1405–1408.
- Blilou, I., Xu, J., Wildwater, M., Willemsen, V., Paponov, I., Friml, J., Heidstra, R., Aida, M., Palme, K., and Scheres, B. (2005). The PIN auxin efflux facilitator network controls growth and patterning in *Arabidopsis* roots. *Nature* **433**: 39–44.
- Bomblies, K., Lempe, J., Epple, P., Warthmann, N., Lanz, C., Dangl, J.L., and Weigel, D. (2007). Autoimmune response as a mechanism for a Dobzhansky-Muller-type incompatibility syndrome in plants. *PLoS Biol.* **5**: e236.
- Borhan, M.H., Holub, E.B., Beynon, J.L., Rozwadowski, K., and Rimmer, S.R. (2004). The *Arabidopsis* TIR-NB-LRR gene RAC1 confers resistance to *Albugo candida* (white rust) and is dependent on EDS1 but not PAD4. *Mol. Plant Microbe Interact.* **17**: 711–719.
- Broman, K.W., Wu, H., Sen, S., and Churchill, G.A. (2003). R/qtl: QTL mapping in experimental crosses. *Bioinformatics* **19**: 889–890.
- Brunoud, G., Wells, D.M., Oliva, M., Larrieu, A., Mirabet, V., Burrow, A.H., Beeckman, T., Kepinski, S., Traas, J., Bennett, M.J., and Vernoux, T. (2012). A novel sensor to map auxin response and distribution at high spatio-temporal resolution. *Nature* **482**: 103–106.
- Caplan, J., Padmanabhan, M., and Dinesh-Kumar, S.P. (2008). Plant NB-LRR immune receptors: From recognition to transcriptional reprogramming. *Cell Host Microbe* **3**: 126–135.
- Chisholm, S.T., Coaker, G., Day, B., and Staskawicz, B.J. (2006). Host-microbe interactions: Shaping the evolution of the plant immune response. *Cell* **124**: 803–814.

- Clarke, J.H., Mithen, R., Brown, J.K.M., and Dean, C. (1995). QTL analysis of flowering time in *Arabidopsis thaliana*. *Mol. Gen. Genet.* **248**: 278–286.
- Colón-Carmona, A., You, R., Haimovitch-Gal, T., and Doerner, P. (1999). Technical advance: Spatio-temporal analysis of mitotic activity with a labile cyclin-GUS fusion protein. *Plant J.* **20**: 503–508.
- Curtis, M.D., and Grossniklaus, U. (2003). A gateway cloning vector set for high-throughput functional analysis of genes in planta. *Plant Physiol.* **133**: 462–469.
- Dello Ioio, R., Linhares, F.S., Scacchi, E., Casamitjana-Martinez, E., Heidstra, R., Costantino, P., and Sabatini, S. (2007). Cytokinin determines *Arabidopsis* root-meristem size by controlling cell differentiation. *Curr. Biol.* **17**: 678–682.
- DeYoung, B.J., and Innes, R.W. (2006). Plant NBS-LRR proteins in pathogen sensing and host defense. *Nat. Immunol.* **7**: 1243–1249.
- Di Laurenzio, L., Wysocka-Diller, J., Malamy, J.E., Pysh, L., Helariutta, Y., Freshour, G., Hahn, M.G., Feldmann, K.A., and Benfey, P.N. (1996). The SCARECROW gene regulates an asymmetric cell division that is essential for generating the radial organization of the *Arabidopsis* root. *Cell* **86**: 423–433.
- Fernández-Marcos, M., Sanz, L., Lewis, D.R., Muday, G.K., and Lorenzo, O. (2011). Nitric oxide causes root apical meristem defects and growth inhibition while reducing PIN-FORMED 1 (PIN1)-dependent acropetal auxin transport. *Proc. Natl. Acad. Sci. USA* **108**: 18506–18511.
- Feys, B.J., Wiermer, M., Bhat, R.A., Moisan, L.J., Medina-Escobar, N., Neu, C., Cabral, A., and Parker, J.E. (2005). *Arabidopsis* SENESCENCE-ASSOCIATED GENE101 stabilizes and signals within an ENHANCED DISEASE SUSCEPTIBILITY1 complex in plant innate immunity. *Plant Cell* **17**: 2601–2613.
- Fonseca, S., Chini, A., Hamberg, M., Adie, B., Porzel, A., Kramell, R., Miersch, O., Wasternack, C., and Solano, R. (2009). (+)-7-iso-Jasmonoyl-L-isoleucine is the endogenous bioactive jasmonate. *Nat. Chem. Biol.* **5**: 344–350.
- Friml, J., Vieten, A., Sauer, M., Weijers, D., Schwarz, H., Hamann, T., Offringa, R., and Jürgens, G. (2003). Efflux-dependent auxin gradients establish the apical-basal axis of *Arabidopsis*. *Nature* **426**: 147–153.
- Fu, Z.Q., Yan, S., Saleh, A., Wang, W., Ruble, J., Oka, N., Mohan, R., Spoel, S.H., Tada, Y., Zheng, N., and Dong, X. (2012). NPR3 and NPR4 are receptors for the immune signal salicylic acid in plants. *Nature* **486**: 228–232.
- Glazebrook, J. (2005). Contrasting mechanisms of defense against biotrophic and necrotrophic pathogens. *Annu. Rev. Phytopathol.* **43**: 205–227.
- Glazebrook, J., Zook, M., Mert, F., Kagan, I., Rogers, E.E., Crute, I.R., Holub, E.B., Hammerschmidt, R., and Ausubel, F.M. (1997). Phytoalexin-deficient mutants of *Arabidopsis* reveal that PAD4 encodes a regulatory factor and that four PAD genes contribute to downy mildew resistance. *Genetics* **146**: 381–392.
- Gómez-Gómez, L., and Boller, T. (2000). FLS2: An LRR receptor-like kinase involved in the perception of the bacterial elicitor flagellin in *Arabidopsis*. *Mol. Cell* **5**: 1003–1011.
- González-García, M.-P., Villarrasa-Blasi, J., Zhiponova, M., Divol, F., Mora-García, S., Russinova, E., and Caño-Delgado, A.I. (2011). Brassinosteroids control meristem size by promoting cell cycle progression in *Arabidopsis* roots. *Development* **138**: 849–859.
- Gray, W.M., Muskett, P.R., Chuang, H.W., and Parker, J.E. (2003). *Arabidopsis* SGT1b is required for SCF(TIR1)-mediated auxin response. *Plant Cell* **15**: 1310–1319.
- Guo, Y.-L., Fitz, J., Schneeberger, K., Ossowski, S., Cao, J., and Weigel, D. (2011). Genome-wide comparison of nucleotide-binding site-leucine-rich repeat-encoding genes in *Arabidopsis*. *Plant Physiol.* **157**: 757–769.
- Heidrich, K., Wirthmueller, L., Tasset, C., Pouzet, C., Deslandes, L., and Parker, J.E. (2011). *Arabidopsis* EDS1 connects pathogen effector recognition to cell compartment-specific immune responses. *Science* **334**: 1401–1404.
- Hu, C.D., and Kerppola, T.K. (2003). Simultaneous visualization of multiple protein interactions in living cells using multicolor fluorescence complementation analysis. *Nat. Biotechnol.* **21**: 539–545.
- Hubbard, K.E., Siegel, R.S., Valerio, G., Brandt, B., and Schroeder, J.I. (2012). Abscisic acid and CO₂ signalling via calcium sensitivity priming in guard cells, new CDPK mutant phenotypes and a method for improved resolution of stomatal stimulus-response analyses. *Ann. Bot. (Lond.)* **109**: 5–17.
- Jones, J.D., and Dangl, J.L. (2006). The plant immune system. *Nature* **444**: 323–329.
- Kadota, Y., Shirasu, K., and Guerois, R. (2010). NLR sensors meet at the SGT1-HSP90 crossroad. *Trends Biochem. Sci.* **35**: 199–207.
- Katoh, K., Misawa, K., Kuma, K., and Miyata, T. (2002). MAFFT: A novel method for rapid multiple sequence alignment based on fast Fourier transform. *Nucleic Acids Res.* **30**: 3059–3066.
- Kim, S.H., Gao, F., Bhattacharjee, S., Adiasor, J.A., Nam, J.C., and Gassmann, W. (2010). The *Arabidopsis* resistance-like gene SNC1 is activated by mutations in SRFR1 and contributes to resistance to the bacterial effector AvrRps4. *PLoS Pathog.* **6**: e1001172.
- Kim, S.H., Kwon, S.I., Saha, D., Anyanwu, N.C., and Gassmann, W. (2009). Resistance to the *Pseudomonas syringae* effector HopA1 is governed by the TIR-NBS-LRR protein RPS6 and is enhanced by mutations in SRFR1. *Plant Physiol.* **150**: 1723–1732.
- Kim, T.-H., et al. (2011). Chemical genetics reveals negative regulation of abscisic acid signaling by a plant immune response pathway. *Curr. Biol.* **21**: 990–997.
- Kubo, M., Udagawa, M., Nishikubo, N., Horiguchi, G., Yamaguchi, M., Ito, J., Mimura, T., Fukuda, H., and Demura, T. (2005). Transcription switches for protoxylem and metaxylem vessel formation. *Genes Dev.* **19**: 1855–1860.
- Lorang, J., Kidarsa, T., Bradford, C.S., Gilbert, B., Curtis, M., Tzeng, S.-C., Maier, C.S., and Wolpert, T.J. (2012). Tricking the guard: Exploiting plant defense for disease susceptibility. *Science* **338**: 659–662.
- Lorenzo, O., Chico, J.M., Sánchez-Serrano, J.J., and Solano, R. (2004). JASMONATE-INSENSITIVE1 encodes a MYC transcription factor essential to discriminate between different jasmonate-regulated defense responses in *Arabidopsis*. *Plant Cell* **16**: 1938–1950.
- Meyers, B.C., Kozik, A., Griego, A., Kuang, H., and Michelmore, R.W. (2003). Genome-wide analysis of NBS-LRR-encoding genes in *Arabidopsis*. *Plant Cell* **15**: 809–834.
- Moreno-Risueno, M.A., Van Norman, J.M., Moreno, A., Zhang, J., Ahnert, S.E., and Benfey, P.N. (2010). Oscillating gene expression determines competence for periodic *Arabidopsis* root branching. *Science* **329**: 1306–1311.
- Nishimura, M.T., Stein, M., Hou, B.H., Vogel, J.P., Edwards, H., and Somerville, S.C. (2003). Loss of a callose synthase results in salicylic acid-dependent disease resistance. *Science* **301**: 969–972.
- Palma, K., Zhao, Q., Cheng, Y.T., Bi, D., Monaghan, J., Cheng, W., Zhang, Y., and Li, X. (2007). Regulation of plant innate immunity by three proteins in a complex conserved across the plant and animal kingdoms. *Genes Dev.* **21**: 1484–1493.
- Park, S.-Y., et al. (2009). Abscisic acid inhibits type 2C protein phosphatases via the PYR/PYL family of START proteins. *Science* **324**: 1068–1071.

- Pedley, K.F., and Martin, G.B.** (2003). Molecular basis of Pto-mediated resistance to bacterial speck disease in tomato. *Annu. Rev. Phytopathol.* **41**: 215–243.
- Raghava, G.P.S., and Barton, G.J.** (2006). Quantification of the variation in percentage identity for protein sequence alignments. *BMC Bioinformatics* **7**: 415.
- Reuber, T.L., Plotnikova, J.M., Dewdney, J., Rogers, E.E., Wood, W., and Ausubel, F.M.** (1998). Correlation of defense gene induction defects with powdery mildew susceptibility in *Arabidopsis* enhanced disease susceptibility mutants. *Plant J.* **16**: 473–485.
- Rietz, S., Stamm, A., Malonek, S., Wagner, S., Becker, D., Medina-Escobar, N., Vlot, A.C., Feys, B.J., Niefind, K., and Parker, J.E.** (2011). Different roles of Enhanced Disease Susceptibility1 (EDS1) bound to and dissociated from Phytoalexin Deficient4 (PAD4) in *Arabidopsis* immunity. *New Phytol.* **191**: 107–119.
- Rogers, E.E., and Ausubel, F.M.** (1997). *Arabidopsis* enhanced disease susceptibility mutants exhibit enhanced susceptibility to several bacterial pathogens and alterations in PR-1 gene expression. *Plant Cell* **9**: 305–316.
- Sangster, T.A., Bahrami, A., Wilczek, A., Watanabe, E., Schellenberg, K., McLellan, C., Kelley, A., Kong, S.W., Queitsch, C., and Lindquist, S.** (2007). Phenotypic diversity and altered environmental plasticity in *Arabidopsis thaliana* with reduced Hsp90 levels. *PLoS ONE* **2**: e648.
- Schmid, M., Davison, T.S., Henz, S.R., Pape, U.J., Demar, M., Vingron, M., Schölkopf, B., Weigel, D., and Lohmann, J.U.** (2005). A gene expression map of *Arabidopsis thaliana* development. *Nat. Genet.* **37**: 501–506.
- Schneider, C.A., Rasband, W.S., and Eliceiri, K.W.** (2012). NIH Image to ImageJ: 25 years of image analysis. *Nat. Methods* **9**: 671–675.
- Schreiber, S.L.** (2000). Target-oriented and diversity-oriented organic synthesis in drug discovery. *Science* **287**: 1964–1969.
- Sheard, L.B., et al.** (2010). Jasmonate perception by inositol-phosphate-potentiated COI1-JAZ co-receptor. *Nature* **468**: 400–405.
- Shen, Q.H., and Schulze-Lefert, P.** (2007). Rumble in the nuclear jungle: Compartmentalization, trafficking, and nuclear action of plant immune receptors. *EMBO J.* **26**: 4293–4301.
- Shirasu, K.** (2009). The HSP90-SGT1 chaperone complex for NLR immune sensors. *Annu. Rev. Plant Biol.* **60**: 139–164.
- Singer, T., Fan, Y., Chang, H.S., Zhu, T., Hazen, S.P., and Briggs, S.P.** (2006). A high-resolution map of *Arabidopsis* recombinant inbred lines by whole-genome exon array hybridization. *PLoS Genet.* **2**: e144.
- Stebbins, C.E., Russo, A.A., Schneider, C., Rosen, N., Hartl, F.U., and Pavletich, N.P.** (1997). Crystal structure of an Hsp90-geldanamycin complex: targeting of a protein chaperone by an antitumor agent. *Cell* **89**: 239–250.
- Sweat, T.A., and Wolpert, T.J.** (2007). Thioredoxin h5 is required for victorin sensitivity mediated by a CC-NBS-LRR gene in *Arabidopsis*. *Plant Cell* **19**: 673–687.
- Thompson, J.D., Thierry, J.C., and Poch, O.** (2003). RASCAL: Rapid scanning and correction of multiple sequence alignments. *Bioinformatics* **19**: 1155–1161.
- Tian, D., Traw, M.B., Chen, J.Q., Kreitman, M., and Bergelson, J.** (2003). Fitness costs of R-gene-mediated resistance in *Arabidopsis thaliana*. *Nature* **423**: 74–77.
- Tornero, P., Merritt, P., Sadanandom, A., Shirasu, K., Innes, R.W., and Dangi, J.L.** (2002). RAR1 and NDR1 contribute quantitatively to disease resistance in *Arabidopsis*, and their relative contributions are dependent on the R gene assayed. *Plant Cell* **14**: 1005–1015.
- Weigel, D.** (2012). Natural variation in *Arabidopsis*: From molecular genetics to ecological genomics. *Plant Physiol.* **158**: 2–22.
- Wiermer, M., Feys, B.J., and Parker, J.E.** (2005). Plant immunity: The EDS1 regulatory node. *Curr. Opin. Plant Biol.* **8**: 383–389.
- Winter, D., Vinegar, B., Nahal, H., Ammar, R., Wilson, G.V., and Provart, N.J.** (2007). An “Electronic Fluorescent Pictograph” browser for exploring and analyzing large-scale biological data sets. *PLoS ONE* **2**: e718.
- Wirthmueller, L., Zhang, Y., Jones, J.D., and Parker, J.E.** (2007). Nuclear accumulation of the *Arabidopsis* immune receptor RPS4 is necessary for triggering EDS1-dependent defense. *Curr. Biol.* **17**: 2023–2029.
- Yang, S., and Hua, J.** (2004). A haplotype-specific Resistance gene regulated by BONZAI1 mediates temperature-dependent growth control in *Arabidopsis*. *Plant Cell* **16**: 1060–1071.
- Yi, H., and Richards, E.J.** (2007). A cluster of disease resistance genes in *Arabidopsis* is coordinately regulated by transcriptional activation and RNA silencing. *Plant Cell* **19**: 2929–2939.
- Zhang, X.-C., and Gassmann, W.** (2007). Alternative splicing and mRNA levels of the disease resistance gene RPS4 are induced during defense responses. *Plant Physiol.* **145**: 1577–1587.
- Zhang, Y., Cheng, Y.T., Qu, N., Zhao, Q., Bi, D., and Li, X.** (2006). Negative regulation of defense responses in *Arabidopsis* by two NPR1 paralogs. *Plant J.* **48**: 647–656.
- Zhang, Y., Goritschnig, S., Dong, X., and Li, X.** (2003b). A gain-of-function mutation in a plant disease resistance gene leads to constitutive activation of downstream signal transduction pathways in suppressor of npr1-1, constitutive 1. *Plant Cell* **15**: 2636–2646.
- Zhang, Y., Tessaro, M.J., Lassner, M., and Li, X.** (2003a). Knockout analysis of *Arabidopsis* transcription factors TGA2, TGA5, and TGA6 reveals their redundant and essential roles in systemic acquired resistance. *Plant Cell* **15**: 2647–2653.
- Ziolkowski, P.A., Koczyk, G., Galganski, L., and Sadowski, J.** (2009). Genome sequence comparison of Col and Ler lines reveals the dynamic nature of *Arabidopsis* chromosomes. *Nucleic Acids Res.* **37**: 3189–3201.
- Zouhar, J., Hicks, G.R., and Raikhel, N.V.** (2004). Sorting inhibitors (Sortins): Chemical compounds to study vacuolar sorting in *Arabidopsis*. *Proc. Natl. Acad. Sci. USA* **101**: 9497–9501.